



Variation in reservoir connectivity in vertically stacked deepwater turbidite channels: impacts on oil recovery

B. A. OMONIYI

Department of Earth Sciences, Adekunle Ajasin University, Akungba – Akoko, Ondo State, Nigeria
E-mail address: bayonle.omoniyi@aaau.edu.ng

Abstract

Keywords:

Turbidite reservoirs, facies, attribute indices, channel forms, reservoir connectivity.

The study demonstrates the influence of variable reservoir connectivity on oil recovery from turbidite reservoir marked by stacked channel architecture. The considerable variability in facies types and distribution affects the geometry and dimensions of sand bodies that make up individual channel forms. The results from the application of attribute indices approach to estimate connectivity of the reservoir facies are pretty consistent with the conceptualised facies distribution across the reservoir system. The vertical stacking pattern of channel-fill facies enables a levee complex to develop. This complex bound up with slope sediments improving lateral connectivity between channel-fill and overbank facies for effective communication between injection well (16/07a-B14) that penetrates the slope facies and production well (16/07a-B1) that penetrates the channel-fill facies. The occurrence of mudstone at the base of individual channel forms reduces vertical connectivity at channel margins. The mudstone distribution constitutes a major risk to vertical oil sweep, particularly in channel-axis, channel-off-axis and channel-margin sequences. In order to optimise oil recovery from deepwater turbidite reservoirs with similar reservoir architecture, it is therefore crucial to consider a depletion strategy that will reduce the risk of differential waterflood performance and improve oil sweep, particularly in the vicinity of production wells.

Accepted: 7 September, 2018 © Science Research Annals. All rights reserved.

1.0 INTRODUCTION

Deepwater plays account for 50% of new discoveries in the last two decades (Stow, 2000; Pettingill, 2004; Hurst *et al.*, 2005), occurring in a wide spectrum of deepwater settings including Gulf of Mexico, offshore West Africa, Brazil, Australia, offshore Northwest Europe, East Africa, and Southeast Asia. Among these plays, turbidites and associated deepwater facies are primary reservoir targets. In the North Sea, over 95% of oil production and 40% of gas production in the last twenty years are from the Palaeogene and Jurassic submarine-fan reservoirs (Glennie, 1984; Richards *et al.*, 1998).

Development of deepwater prospects is hugely expensive (OfurhieandOkpere, 2002). In offshore Nigeria, development costs for Bonga, Erha and Erha North, Yoho, and Agbami fields range between \$1.3 and \$3.5 billion (Offshore Technology, 2000; Igbikiowubo, 2003; Ludot and Delattre, 2010; Rafin and Laine, 2010). In particular, the cost of drilling the first wells at Agbami field range between \$60 million and \$90 million. Other fields that have deepwater reservoirs in offshore Nigeria include Akpo, Doro, Bosi, Abo, Chota, Bolia, Ebwa, Nnwa, Aparo, Sonam, Ikija, Nsiko, and Ngolo fields. The successful development of some of these fields resulted in the

discovery of satellite fields, which upon successful development were tied to the production platform to maximise production and to delay production decline. The Chevron-operated Agbami field and Shell-operated Bonga field are two classic examples. The 182 km²-Agbami field, which first encountered 420 ft of net pay in Agbami-1 well has been a major success in deepwater field development. Coming on stream in 2008, the field has estimated original oil-in-place of 900 MMbbl (Grimes *et al.*, 2004; Hollister and Spokes, 2004; Odusote, 2013). With peak oil production of 250,000 bbl/d (2009), the field is improving recovery through the development of Agbami Phase 3 project, in spite of difficulty in reservoir characterisation experienced during the early stages of development.

The field development plan for Bonga field, like Agbami field, has also resulted in tremendous success. Oil production from middle to late Miocene unconsolidated turbidite sandstones in channel reservoirs increased from 200,000 bbl/d in 2006 to 225,000 bbl/d in 2017 with a cumulative oil production of 280 MMbbl (Inikori *et al.*, 2009; Shell, 2011; Zhang *et al.*, 2013; Offshore Technology, 2015). The success of the development strategy, which led to the discovery of two satellite fields: Bonga SW (2001) and Bonga North (2004), is not unconnected with early understanding of key parameters that impact fluid flow. Among these parameters are net sand distribution, sub-seismic channel architecture and reservoir connectivity (Chapin *et al.*, 2002). As a result of the complexity of channelised turbidite reservoirs, inadequate understanding of these parameters may spring up unpleasant surprises such as failure to deliver promised rates and profiles. For example, in the Eni-operated Oyo field, the discovery in Pliocene turbidite reservoir (Adenipekun *et al.*, 2017), which was considered uncommercial by Statoil in 1996, has not performed up to production expectations. Less than one year after first oil, early gas breakthrough caused decline in oil production rate from 22,000 bbl/d to 6,000 bbl/d. The situation is only being remedied by a series of intervention operation (Vanguard, 2010; This Day, 2011, 2014).

Channel-levee systems are the primary architectural element that is associated with large submarine fans (Twichell *et al.*, 1991; Kenyon *et al.*, 1995; Kolla and Schwab, 1995; Pirmez and Flood, 1995; Schwenk *et al.*, 2003). Erosionally confined deepwater channel complexes form important

reservoirs in deep offshore Nigeria. Within these systems, fluid flow is often more complex than expected (Labourdet *et al.*, 2006) because (lateral and vertical) connectivity within such systems is extremely variable. This paper, therefore, showcases the results from the application of a novel quantitative approach to assess variation in connectivity of reservoir facies in stacked deepwater turbidite channels and to evaluate the implications of this variation on oil recovery.

The study area, North Brae field, is part of a cluster of fields, which are located in the western margin of the South Viking Graben (Figure 1) in the United Kingdom Continental Shelf.

2.0 GEOLOGY OF THE NORTH BRAE FIELD

The North Brae field is 19 km² in area. It has average net-to-gross ratio of 0.85 and produces condensate and dry gas from the Brae reservoir within the Upper Jurassic Brae system (Figure 2). The reservoir is 700-m thick and consists of 169-m thick hydrocarbon column, which is trapped in its three-way structural dip closure and sealed by the Kimmeridge Clay Formation. Recoverable hydrocarbon in the field is estimated to be 207 MMbbl of condensate and 800 Bcf of dry gas (Stephenson, 1991; Brehm, 2003).

In contrast to previous interpretations by Harms *et al.* (1981), Stow (1984c) and Stow *et al.* (1982) considered the Brae system to be a deepwater turbidite system comprising overlapping slope-apron fans, which are characterised by interdigitating conglomerate and sandstone turbidites that form part of a larger turbidite system. The sediments in this system were sourced from the Fladen Ground Spur, which is located west of the basin, and transported by alluvial fans and high-energy rivers to feed the basin via a west-east trending channel-fill complex (Figure 3). The complex, largely made up of conglomerates and sandstones, is flanked by thin (TBT; 3-10 cm thick sand/silt unit) and very thin (VTBT; <3 cm thick sand/silt unit) sandstone-mudstone interbeds (Omoniyi *et al.*, 2018).

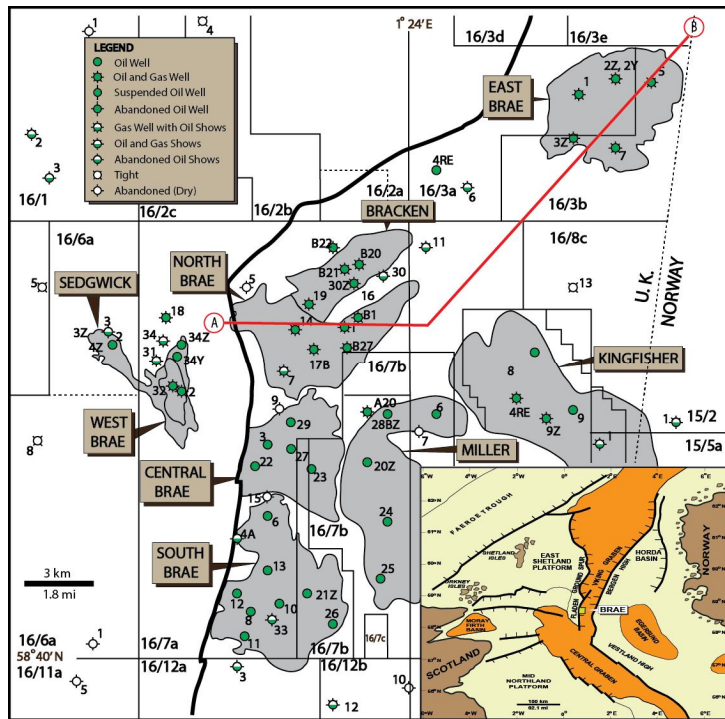


Figure 1. A map showing cluster of Brae fields within the context of regional structural setting (South Viking Graben, inset). Figure adapted from Omoniye *et al.* (2018).

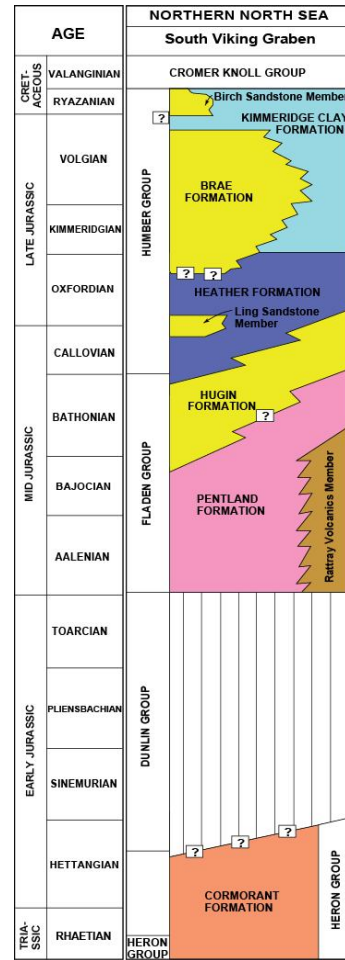


Figure 2. Lithostratigraphic chart of the South Viking Graben, Northern North Sea (from Omoniye *et al.*, 2018).

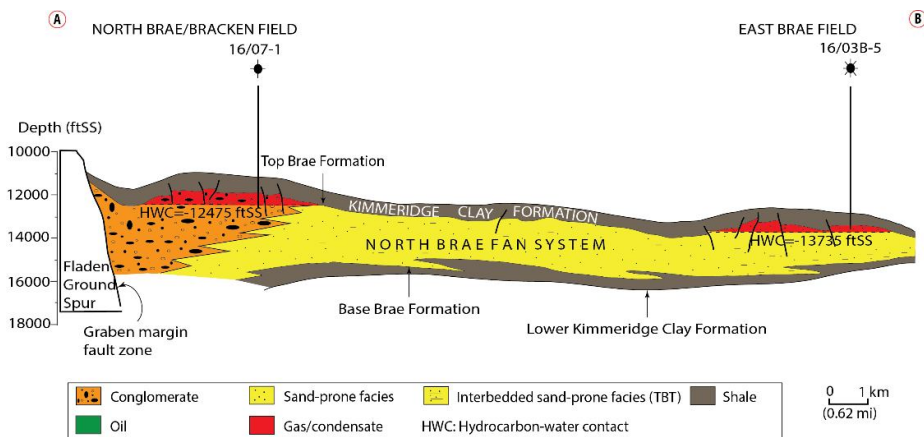


Figure 3. Schematic cross section from margin to basin along line A-B in Figure 1, illustrating the geometry of the Upper Jurassic Brae submarine fan system at the North Brae field (from Omoniye *et al.*, 2018).

3.0 METHODS

3.1 Sediment facies and correlation

Facies type and distribution considerably vary in deepwater systems (Tudor, 2014). Tenwells comprising 16/07a-1, 16/07a-19, 16/07a-B1, 16/07a-B7, 16/07a-B8, 16/07a-B9, 16/07a-B10, 16/07a-B14, 16/07a-B17 and 16/07a-B27 were used for this study. From these wells, 16/07a-B1, 16/07a-B10 and 16/07a-B14, marked by 85-100% core recovery, were examined for sediment facies description and core-integrated well correlation. In order to capture the level of heterogeneity adequate for flow simulation, four main sediment facies associations are recognised in the North Brae field (Omoniyi, 2017). These facies are:

- i. **FA1_{NEF}**: The facies association comprises silty/sandy mudstone. Average siltstone/sandstone <20%. Beds are <5 cm thick.
- ii. **FA2_{NEF}**: **FA2_{NEF}** is composed of shaly/silty sandstone. It is characterised by variable bed thickness, usually <10 cm, and average sand content between 50% and 60%.
- iii. **FA3_{NEF}**: Although this facies association is composed of sandstone in its entirety, thin mudstone layers may occur to separate individual beds. Characterised by very well sorting, **FA3_{NEF}** has very good visible porosity. Beds are generally over 5 cm thick.
- iv. **FA4_{NEF}**: The facies association consists of conglomerate with sandstone clasts of variable sizes, which may occur as blocky pebbles and cobbles. It is clast-supported. Mudstone clasts account for <5% of clast population.

For facies correlation, wells were spaced using information from Brae Formation top structure map, and were aligned to the top of the formation. Correlation enabled layering, which captured the size of the grid cell. The resultant lithostratigraphic scheme (Figure 4) provided input parameters for subsequent three-dimensional modeling. By this approach, critical uncertainty that concerned thickness and lateral continuity of reservoir facies, particularly within heterolithic intervals was effectively reduced.

As observed in the lithostratigraphic scheme (see Figure 4), channel-fill sequence comprising

FA4_{NEF} passes upwards into an interval of **FA3_{NEF}**, which also extends to the overbank to develop a levee complex. Bound by slope sediments, the sequence is topped by **FA2_{NEF}**. Each distinctive channel-thalweg displays a systematic change in proportion of conglomerate to sand-rich facies, bed architecture, and sandstone geometry from channel axis to channel-off-axis and to channel margin. Within the multi-storey architecture, lateral variation in facies from channel axis through channel margin to overbank is noticeable. The channel-fill succession in the thalwegs has a marked thinning and fining-upward trend. The channel margin-to-overbank setting, by contrast, is characterised by a thickening- and coarsening-upward trend.

3.2 Attribute indices

Good communication between injection well and production well is vital for economic recovery of hydrocarbon fluid from turbidite reservoirs. Omoniyi *et al.* (2013) combined the geological attributes of turbidite facies to develop four attribute indices. These indices are: *facies* Net-to-Gross Index (NGI), Sand Connectivity Index (SCI), Facies Ratio Index (FRI), and Sediment Textural Index (STI). These indices can be used to characterise very thin and thin-bedded turbidite facies and associated thicker-bedded turbidite facies. The indices serve as a quantitative tool that can be used to discriminate between deepwater architectural elements. For the present study, only NGI and SCI are further explored. The following sub-sections provide a summary from Omoniyi (2017).

3.2.1 Facies Net-to-Gross Index (NGI)

The NGI expresses the standard net to gross sand value that is widely used to evaluate reservoir intervals. It is expressed as:

$$NGI = \left[\frac{(NT)_f}{(GT)_f} \right] \quad (1)$$

(NT)_f is the net thickness of a particular facies association under consideration, and **(GT)_f** is the gross thickness of the entire interval under consideration.

NGI varies from 0 to 1. For a specific facies association, low NGI values imply low net-to-gross, whereas high NGI values indicate high net-to-gross.

3.2.2 Vertical Connectivity Index (VCI)

VCI indicates the apparent vertical connectivity of TBT/VTBT facies associations and related sand bodies. It is a product of *facies* Net-to-Gross Index and Vertical Connectivity Factor. That is:

$$VCI = NGI \times VCF \tag{2}$$

NGI is defined in Equation 1 and VCF is calculated as follows:

$$VCF = \left[\frac{S/S}{(S/S + S/NS)} \right] \tag{3}$$

where S/S is the proportion of sand overlying sand, and S/NS represents the proportion of sand overlying non-sand or non-silt lithology.

VCI varies from 0 to 1. Low VCI values indicate low apparent vertical connectivity and high VCI values reflect high apparent vertical connectivity.

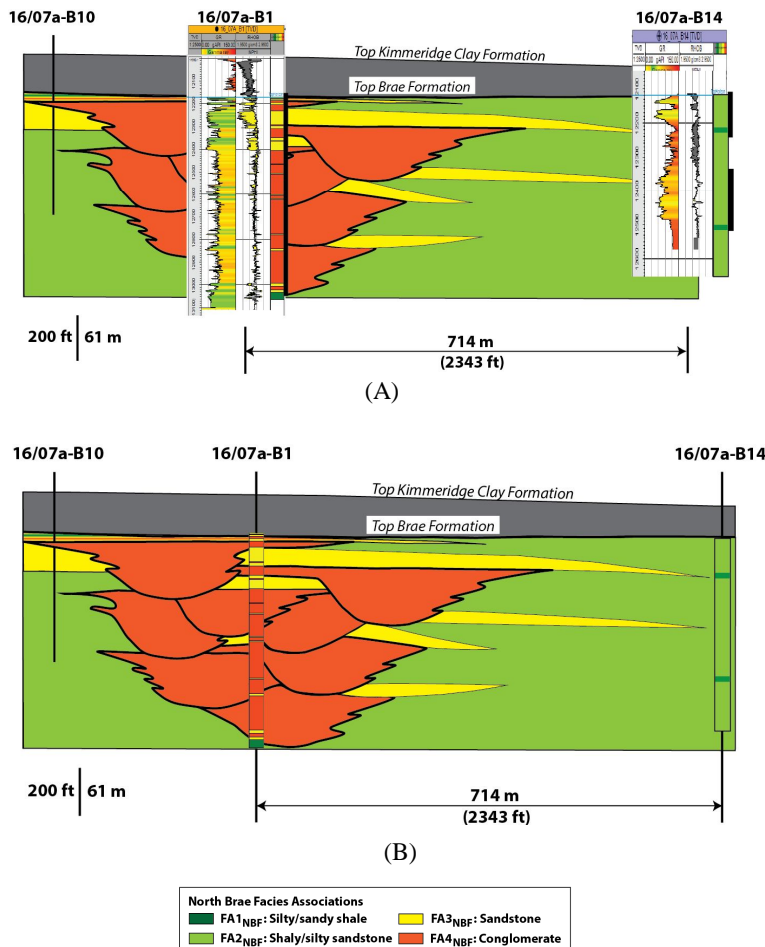
Figure4. (A) Core-integrated well correlation based on interpretation of gamma logs. Black thick lines indicate cored intervals. (B) Lithostratigraphic scheme based on sand bodies within the interval being considered.

It is expressed as:

$$LCI = \left[\frac{(h_1/X) \times n_1}{(h_2/X) \times n_2} \right] \tag{4}$$

where h_1 and h_2 are interval thicknesses at two locations (1 and 2); X is distance between the two locations; and n_1 and n_2 represent number of beds within the interval under consideration at locations 1 and 2, respectively.

LCI varies from 0 to 1. Low LCI values indicate low apparent lateral connectivity and high LCI values represent high apparent lateral connectivity.



3.2.4 Sand Connectivity Index (SCI)

The Sand Connectivity Index is a measure of the spatial connectivity within an interval of TBT/VTBT facies association or associated turbidite sand bodies. Unlike pressure data, well-test data, and production data, which are indirect methods for estimating connectivity between fluid contacts or between injection well and production well, SCI-derived connectivity is based on the nature of bed/lamination cross-cutting relationships, which is calculated using Equation 5:

$$SCI = \frac{1}{2} (VCI + LCI) \times NGI \quad (5)$$

NGI refers to *facies* Net-to-Gross Index, VCI is Vertical Connectivity Index, and LCI is Lateral Connectivity Index (see Equations 1-4).

3.3 Grid design and property distribution

Three-dimensional models are necessary to reflect the internal structure of reservoirs for reliable flow simulation (Szerbiak, 2001). In this study, definition of geological layers reflects the resolution that is adequate to capture the scale of heterogeneity of interest yet without losing geological details. The grid comprises 197,800 cells, and is characterised by corner-point geometry. Down-gridding approach using geological considerations guided by core-integrated well correlation was adopted.

Core-calibrated well logs from 16/07a-B1 and 16/07a-B14 were interpreted to generate a facies log apiece. The facies property was upscaled using *most of* averaging method, which allowed the most abundant lithology type in a cell to represent it. The inter-well sector considered for this study cover the area between 16/07a-B1 and 16/07a-B14 (see Figure 4). Channel dimensions extracted from the lithostratigraphic scheme (Table 1) served as input parameters for the object model. The porosity and permeability properties were modeled based on facies-conditioned Sequential Gaussian Simulation approach.

4.0 RESULTS

4.1 Facies attribute indices

The success of a depletion strategy that is based on waterflooding is largely influenced by the degree of communication between injection wells and production wells, which is a function of connectivity of reservoir facies. In particular, productivity is

improved when injected water provides pressure support and influences oil sweep. The effectiveness of the connectivity pathways depends on the proportion of sand bodies that connect together. The attribute indices approach is a tool that can be used to validate flow simulation models, thus reducing uncertainty that is associated with connectivity at inter-well spacing.

From the attribute indices obtained for this study, NGI, VCI and LCI are 0.98,0.92 and 0.32, respectively. These values correspond to SCI of 0.61.

Table 1. Channel dimensions that serve as input parameters for facies modeling.

Property	Value
Width	250-350 m
Thickness	85 m
Width-to-thickness ratio	~3:1 – 4:1

4.2 Property models

The spatial distribution of the constituent facies associations (hereafter referred to as ‘facies’ for convenience) in the conceptualised facies distribution map (Figure 5) is shown in Figure 6A. Figure 6B reflects the variation in net-to-gross (NTG) property in the sector considered. Overall, NTG is highest in **FA3_{NTG}** and lowest in **FA1_{NTG}**. This trend is observed for porosity and permeability distributions across the sector (Figure 7).

4.3 Flow simulation

The simulation of the three-dimensional property models was performed using a depletion strategy that utilised waterflooding for pressure support and oil sweep. Water was injected into 16/07a-B14 at a constant rate of 20,000 bbl/d. Oil production rate, 20,000 bbl/d, was kept constant for the period of production, which lasted for 5 years.

From the simulation results, cumulative oil production and recovery efficiency, and oil production rate and decline are discussed as follows:

4.3.1 Cumulative oil production and recovery efficiency

From the simulation, it was observed that 12.6 MMbbl of oil was produced at 25% recovery efficiency prior to water breakthrough (734 days). At the end of five years, recovery efficiency increased to

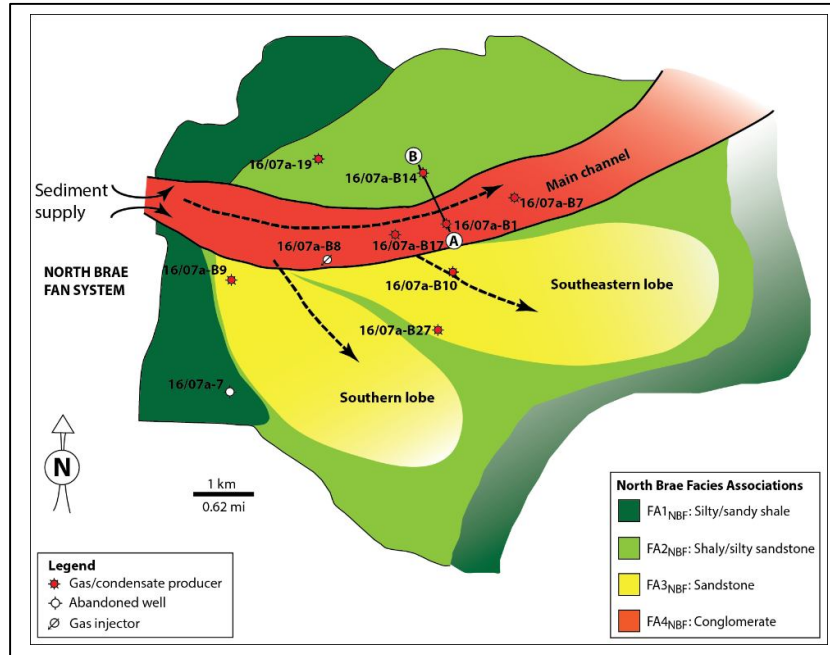


Figure 5. Facies distribution map for the North Brae field, showing distribution of primary facies in the Upper Brae Formation (from Omoniyi, 2017). The black solid line A-B is the sector considered for this study.

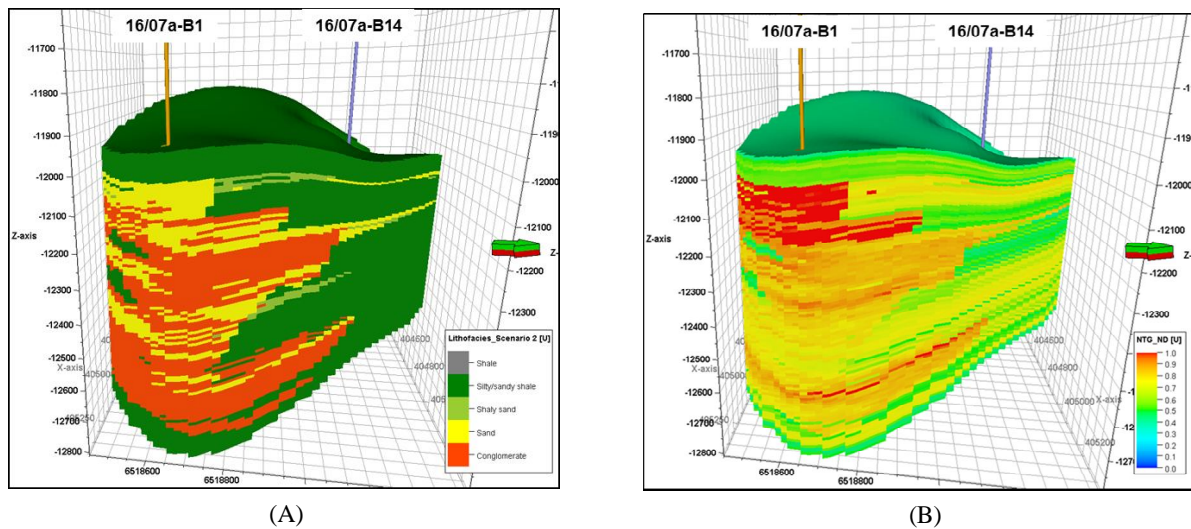


Figure 6. Three-dimensional models showing distribution of (A) principal facies, and (B) net-to-gross between 16/07a-B1 and 16/07a-B14. The net-to-gross model was generated from combined neutron and density logs, which were interpreted to define volume of shale, and then, to derive net-to-gross property.

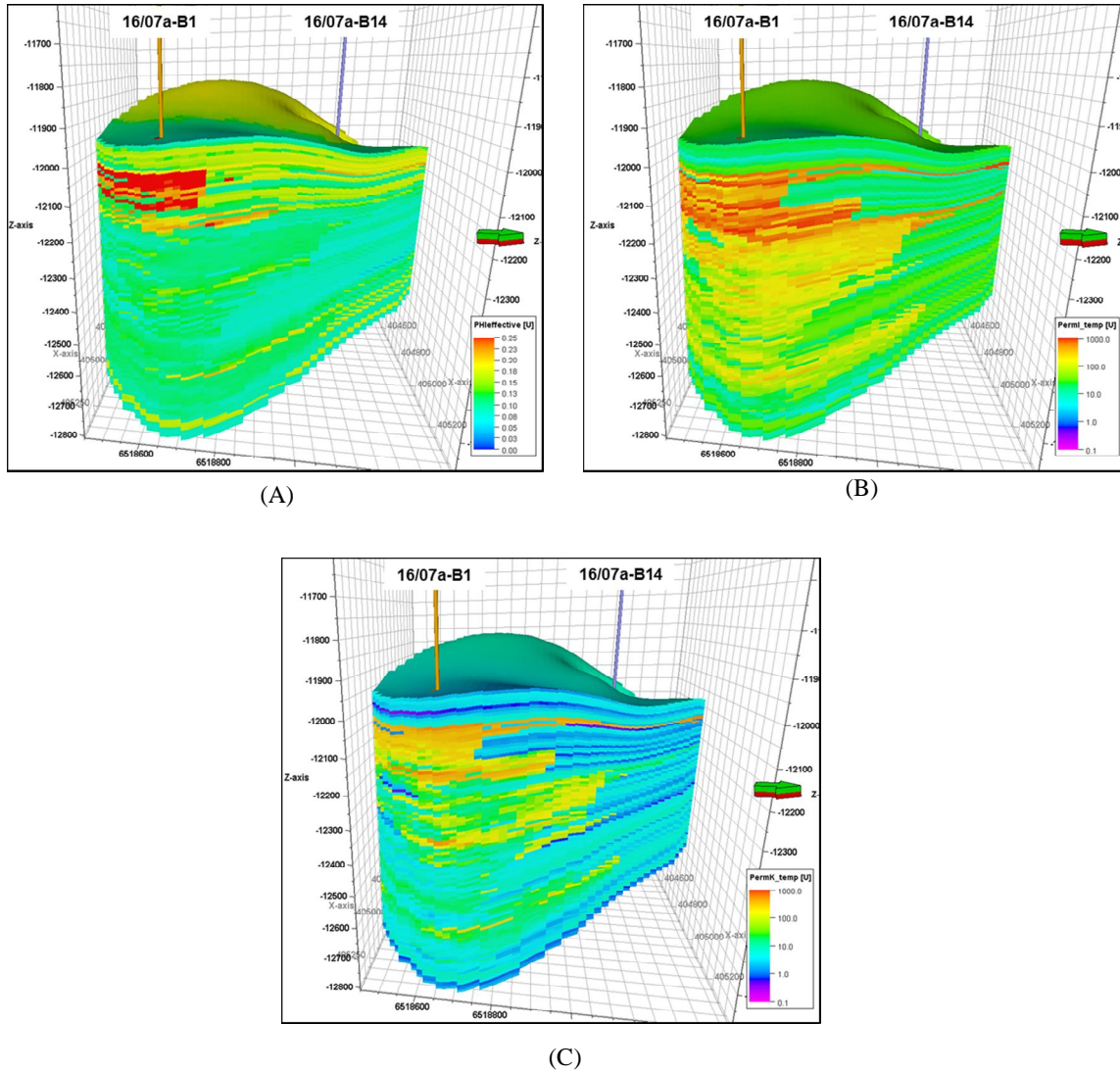


Figure 7. Three-dimensional models showing distribution of (A) porosity, (B) horizontal permeability, and (C) vertical permeability between 16/07a-B1 and 16/07a-B14.

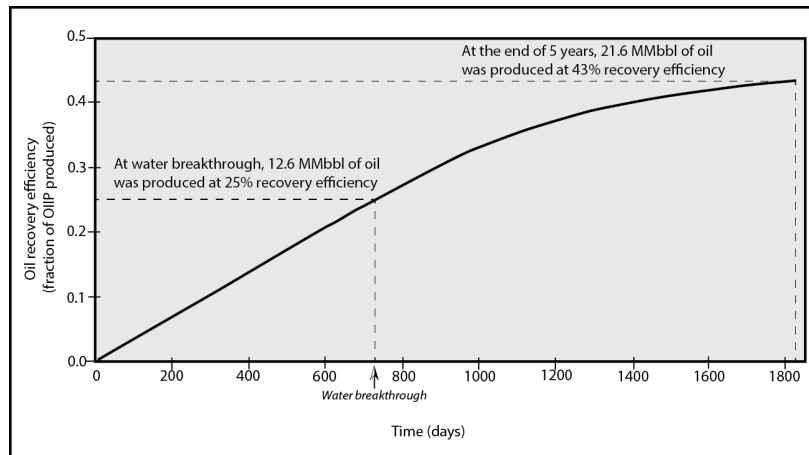


Figure 8. Oil recovery efficiency profile over five years of production for the sector of North Brae field considered.

43% with a corresponding increase in cumulative oil production to 21.6 MMbbl (Figure 8).

4.3.2 Oil production rate and decline

Oil production rate profile for stacked turbidite channels considered for this study is presented in Figure 9. From the profile, a rapid decline in oil production rate from 17,120 bbl/d (at start-up) to 2,936 bbl/d (at the end of 5 years) can be clearly observed. The decline in rate is connected to breakthrough of injected water at the production well (16/07a-B1).

5.0 DISCUSSION

5.1 Reservoir architecture and facies attributes

Reservoir architecture impacts pore volume (Larue and Friedmann, 2005) and its influence on fluid displacement. As a result of the non-uniform spatial distribution of net sand, which serves as flow conduits, uncertainty in oil recovery is enhanced in channel-levee systems (Sylvester *et al.*, 2011). This uncertainty is occasioned by regular and irregular low net-to-gross facies, which occur within channel axis, off-axis-to-channel-margin and overbank settings. The variation in attribute indices (NGI, VCI, LCI and SCI) of reservoir facies within these settings impacts oil displacement process from injection well to production well.

Turbidite reservoirs that are characterised by multi-storey architecture may comprise channel forms that have mud-lined margins, which may reduce vertical connectivity within a channel-fill succession. The sandstone packages within each fill, however, may extend beyond its margin to form a levee in the overbank (Cronin *et al.*, 2000). Amalgamation of such levees will develop into a vertically-stacked levee complex, enabling laterally and vertically connected flow pathways. As observed during simulation, these pathways encouraged effective oil displacement from the injection well to the production well.

The impact of lower net-to-gross and lower connectivity in the bounding slope system on oil recovery is ameliorated by the amalgamated stacking of channel-fill and levee strata, allowing injected water to sweep most parts of the system as it displaced oil in the sand-rich levees into individual channel fills.

5.2 Reservoir connectivity and oil sweep

Variation in attribute indices of reservoir facies has profound influence on their dynamic behaviour. As observed from the results, the SCI-derived connectivity is relatively uniform between the injection and production wells. In contrast to the SCI profile, the marked drop in VCI profile caused differential oil displacement within 221 m (725 ft)-radius of the production well (Figure 10). As a result of the lower VCI in the vicinity of the production well, injected water preferentially swept the middle-to-upper part of the system while the lower part lagged behind in terms of oil sweep (Figure 11A). In spite of intermediate lateral connectivity (LCI=0.41) in this region, much of the oil in the middle-to-lower section of the system was largely unswept prior to water breakthrough (Figure 11B).

5.3 Reservoir performance

Predicting reservoir performance using integrated earth models that are developed from robust subsurface data is key to successful development planning (Chapin *et al.*, 2002). As observed for the stacked channel architecture considered for this study, variable attribute indices caused significant decline in oil production, particularly within intervals of low vertical connectivity near the production well. The reservoir architecture allowed rapid decline in oil production rate after breakthrough of injected water (see Figure 9). In turbidite reservoirs marked by this architectural style, oil production suffers at high production rate resulting in progressive rapid production decline, increase in water production, and much lower cumulative oil production in the long term.

6.0 CONCLUSIONS

Reservoir connectivity is directly related to facies type and spatial distribution. The results presented in this study indicate that reservoir connectivity influences oil displacement process, which is largely dependent on permeability contrast in deepwater channel reservoirs. This contrast is enhanced by variation in geometrical shape and continuity of reservoir facies. The variables, as observed from the results, adversely affected the connectivity of flow conduits and resultant oil production rates and decline. It is therefore important to consider a depletion strategy that will reduce the risk of flow fingering and improve oil sweep in the vicinity of the production well.

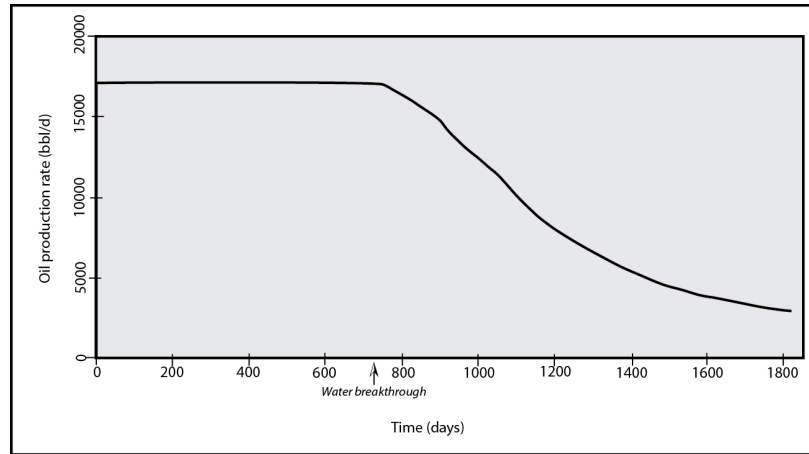


Figure 9. Oil production rate profile over five years of production for the sector of North Brae field considered. Water breakthrough has adverse effect on oil production rate causing its rapid decline.

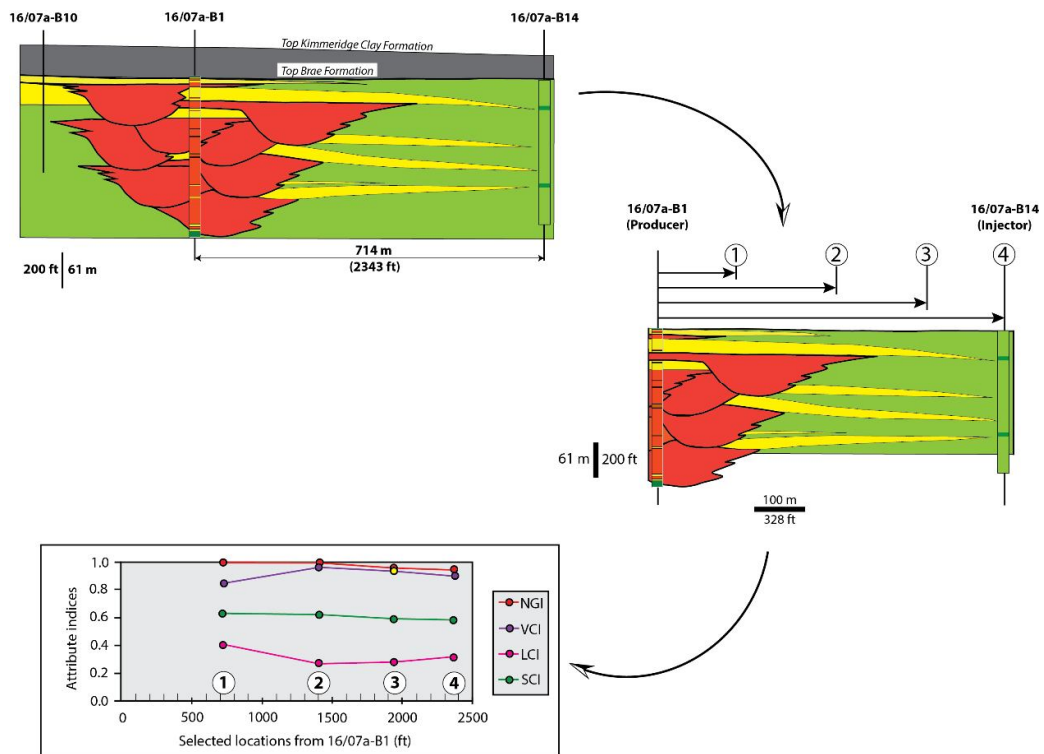
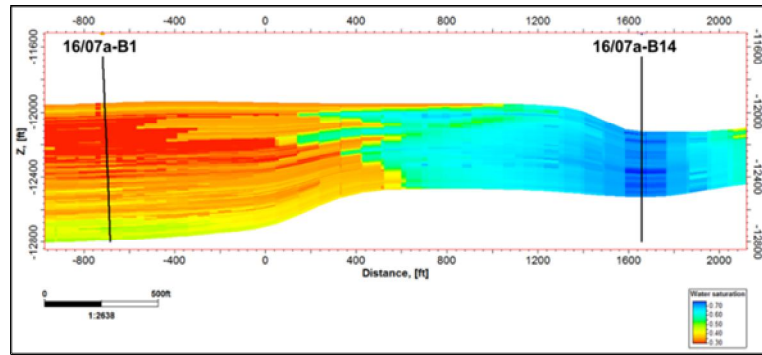
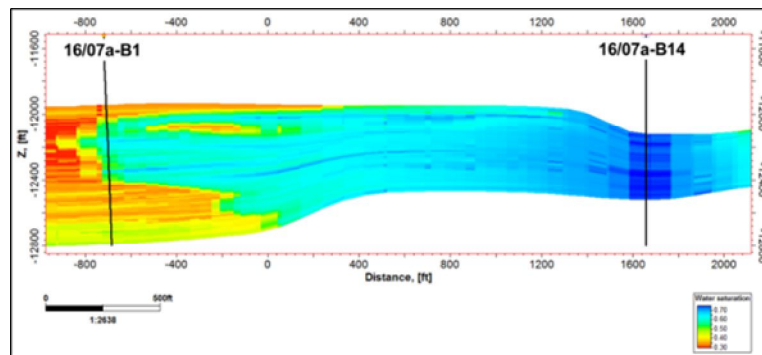


Figure 10. Schematic diagrams and chart showing variation in attribute indices of reservoir facies between 16/07a-B1 and 16/07a-B14 as a function of distance (locations 1-4) from the production well. (1) 725 ft (221 m), (2) 1405 ft (428 m), (3) 1935 ft (590 m), and (4) 2365 ft (721 m). Although SCI profile is relatively uniform, greater variation is implied from LCI and VCI profiles.



(A)



(B)

Figure 11. Comparison of water displacement process in relation to oil production in the sector of North Brae field considered: (A) 244 days, and (B) 609 days after start-up.

ACKNOWLEDGEMENTS

This study is part of the author's PhD thesis, which was sponsored by the Tertiary Education Trust Fund (TETFUND). The author is immensely grateful to TETFUND. The anonymous reviewers are very much appreciated for their constructive comments.

REFERENCES

Adenipekun, A., G. Marinho, O. Odeyemi, C. Ugboaja, A. Basse, and E. Nnnebocha, 2017. Riserless light well intervention restores production on Oyo-8 subsea well. Offshore Technology Conference, Houston, May 1-4, 10 p.

Arps, J. J., 1945. Analysis of decline curves. Transactions of the AIME 160: 228-247.

Brehm, J. A., 2003. The North Brae and Beinn Fields, Block 16/7a, UK North Sea. In: J. G. Gluyas and H. M. Hitchens, eds., United Kingdom Oil and Gas Fields, Commemorative Millennium Volume Geological Society, London, 199-209

Chapin, M., P. Swinburn, R. Weiden, D. Skaloud, S. Adesanya, D. Stevens, C. Varley, and J. Wilkie, 2002. Integrated seismic and subsurface characterization of Bonga Field, offshore Nigeria. The Leading Edge, 1125-1131.

Cronin, B. T., A. Hurst, H. Celik, and I. Türkmen, 2000. Superb exposure of a channel, levee and overbank complex in an ancient deep-water slope environment. *Sedimentary Geology*, 132, 205-216.

Glennie, K. W., 1984. Introduction to the Petroleum Geology of the North Sea. Blackwell Scientific Publications, 236 p.

Grimes, D. L., R. M. Cupich, and D. M. Angstadt, 2004. Issues in the use of seismic data at Agbami field, offshore Nigeria. Offshore Technology Conference, Houston, May 3-6, 11 p.

Harms, J. C., P. Tackenberg, E. Pickles, and R. E. Pollock, 1981. The Brae Oilfield Area. In: L. V.

- Illing and G. D. Hobson, eds., *Petroleum Geology of the Continental Shelf of North-West Europe* Institute of Petroleum, Heyden, London, 352-357.
- Hollister, H. D., and J. J. Spokes, 2004. The Agbami project: a world class deepwater development. *Offshore Technology Conference 16987*, Houston, May 3-6, 14 p.
- Hurst, A., A. J. Fraser, S. I. Fraser, and F. Hadler-Jacobsen, 2005. Deep-water clastic reservoirs: a leading global play in terms of reserve replacement and technological challenges. In: A. G. Dore and B. A. Vining, eds., *Petroleum Geology: North-West Europe and Global Perspectives-Proceedings of the 6th Petroleum Geology Conference Geological Society*, London, 1111-1120.
- Igbikiowubo, H., 2003. Nigeria: Bonga, World's largest oil production vessel arrives Nigeria in November. *Vanguard*, Nigeria, Edition 14 October, 2003.
- Inikori, S. O., B. Coxe, E. Ageh, and J. Van Der Bok, 2009. Development of world-class oil production and water injection rate and high ultimate-recovery wells in deepwater turbidites: Bonga Example. *SPE* 110360, 293-302.
- Kenyon, N.H., A. Amir, and A. Cramp, 1995. Geometry of the younger sediment bodies of the Indus Fan. In: K. T. Pickering, R. N. Hiscott, N. H. Kenyon, F. Ricci Lucchi, and R. D. A. Smith, eds., *Atlas of Deep Water Environments: Architectural Style in Turbidite Systems*. Chapman and Hall, London, 89-93.
- Kolla, V., and A. M. Schwab, 1995. Indus Fan: multi-channel seismic reflection images of channel-levee-overbank complexes. In: K. T. Pickering, R. N. Hiscott, N. H. Kenyon, F. Ricci Lucchi, and R. D. A. Smith, eds., *Atlas of Deep Water Environments: Architectural Style in Turbidite Systems*. Chapman and Hall, London, 100-104.
- Labourdet, R., J. Poncet, J. Seguin, F. Temple, J. Hegre, and A. Irving, 2006. Three-dimensional modelling of stacked turbidite channels in West Africa: impact on dynamic reservoir simulations. *Petroleum Geoscience*, 12, 335-345.
- Larue, D. K., and F. Friedmann, 2005. The controversy concerning stratigraphic architecture of channelized reservoirs and recovery by waterflooding. *Petroleum Geoscience* 11: 131-146.
- Ludot, B., and E. Delattre, 2010. Drilling Akpo: 22 wells required, 22 wells delivered for production start-up and plateau. *Offshore Technology Conference 20992*, Houston, May 3-6, 9 p.
- Odusote, F., 2013. Deepwater Nigeria field development: challenges, best practices and lessons learned from the Agbami field. *SPE* 167534, 10 p.
- Offshore Technology, 2000 [Online]. <https://www.offshore-mag.com/articles/print/volume-60/issue-5/news/general-interest/shells-bonga-ea-development-deepwater-renew-interest-off-nigeria.html>
- Offshore Technology, 2015 [Online]. Bonga Deepwater Project, Niger Delta, Nigeria. <http://www.offshore-technology.com/projects/bonga/>
- Ofurhie, M., and K. Okpere, 2002. Nigeria Deep Offshore: Appraisal of Activities from 1991-2001 and Future Challenges. *Proceeding of the 17th World Petroleum Congress*, September 1-5, Rio de Janeiro, Brazil, 7-16.
- Omoniyi, B. A., 2017. Thin-bedded turbidites and channel sands: the connectivity bridge. Unpublished PhD Thesis, Heriot-Watt University, Edinburgh, United Kingdom, 384 p.
- Omoniyi, B. A., D. A. V. Stow, and A. Gardiner, 2013. Thin-bedded turbidites: a new approach toward better characterisation [Abstract]. *52nd BSRG Annual Meeting*, Hull, 64:124.
- Omoniyi, B. A., D. A. V. Stow, and A. Gardiner, 2018. Characterization of thin-bedded turbidites in the North Brae Field, South Viking Graben, North Sea. In: C. C. Turner and B. T. Cronin, eds., *Rift-related coarse-grained submarine fan reservoirs; the Brae Play, South Viking Graben, North Sea: AAPG Memoir 115*, DOI Number: 10.1306/13652184M1153811.
- Pettingill, H., 2004. Global overview of deepwater exploration and production. In: P. Weimer and R. M. Slatt, eds., *Petroleum systems of deepwater settings*

- Society of Exploration Geophysicists*, Oklahoma, 19-56.
- Pirmez, C., and R. D. Flood, 1995. Morphology and structure of Amazon channel. In: R. D. Flood, D. J. W. Piper, A. Klaus, *et al.*, eds., *Proceedings of the OPP, Initial Reports*, 155. Ocean Drilling Program, College Station, Texas, 23-45.
- Rafin, F., and A. Laine, 2010. Akpo: early completion of a giant Nigerian deep offshore development. *Offshore Technology Conference 2009*, Houston, May 3-6, 8 p.
- Richards, M., M. Bowman, and H. Reading, 1998. Submarine-fan systems I: characterization and stratigraphic prediction. *Marine and Petroleum Geology* 15: 689-717.
- Schwenk, T., V. SpieB, C. Hübscher, and M. Breitzke, 2003. Frequent channel avulsions within the active channel-levee system of the middle Bengal Fan: an exceptional channel-levee development derived from Parasound and Hydrosweep data. *Deep-sea Research II*, 50, 1023-1045.
- Shell (Nigeria), 2011. Bonga deep water project. Unpublished Internal Report, 2 p.
- Stephenson, M. A., 1991. The North Brae Field, Block 16/7a, UK North Sea. In: I. L. Abbotts, ed., *United Kingdom Oil and Gas Fields 25 Years Commemorative Volume Geological Society*, London, Avon, 43-48.
- Stow, D. A. V., 1984c. Upper Jurassic overlapping-fans slope-apron system: Brae oilfield, North Sea. *Geo-Marine Letters* 3: 217-222.
- Stow, D. A. V., 2000. Thin-bedded turbidites and associated facies: their nature, geometry and reservoir properties. In: C. J. Appi, ed., *Deep-water sedimentation: technological challenges for the next millennium Brazilian Association of Petroleum Geologists*; *Petróleo Brasileiro*, 40-41.
- Stow, D. A. V., C. D. Bishop, and S. J. Mills, 1982. Sedimentology of the Brae oilfield, North Sea: fan models and controls. *Petroleum Geology* 5: 19.
- Sun, H., ed., 2015. *Advanced production decline analysis and application*. Elsevier Inc., Oxford, 328 p.
- Sylvester, Z., C. Pirmez, and A. Cantelli, 2011. A model of submarine channel-levee evolution based on channel trajectories: implications for stratigraphic architecture. *Marine and Petroleum Geology* 28: 716-727.
- Szerbiak, R.B., G. A. McMechan, R. Corbeanu, and C. Foster, 2001. 3-D characterization of a clastic reservoir analog: from 3-D GPR data to a 3-D fluid permeability model. *Geophysics* 66, 1026-1037.
- This Day, 1 February, 2011. Nigeria: Oyo well-Camac completes intervention operation.
- This Day, 24 June, 2014. Nigeria: CAMAC's Oyo-8 well to commence production in Fourth Quarter.
- Tudor, E. P., 2014. Facies variability in deep water channel-to-lobe transition zone: Jurassic Los Molles Formation, Neuquen Basin, Argentina. Unpublished M. S. Thesis, University of Texas at Austin, 76 p.
- Turner, C. C., J. M. Cohen, E. R. Connell, and D. M. Cooper, 1987. A depositional model for the South Brae oilfield. In: J. Brooks and K. W. Glennie, eds., *Petroleum Geology of North west Europe Graham and Trotman*, London, 856 p.
- Twichell, D.C., N. H. Kenyon, L. Parson, and B. A. McGregor, 1991. Depositional Patterns of the Mississippi Fan Surface: evidence from Gloria II and high-resolution seismic profiles. In: P. Weimer and M. H. Link, eds., *Seismic Facies and Sedimentary Processes of Submarine Fans and Turbidite Systems*. Springer, New York, 349-363.
- Vanguard, 13 December, 2010. CAMAC: Early commencement of Oyo well intervention.
- Zhang, M., J. J. Lee, S. Xu, J. Molyneux, T. Garfield, R. Lovell, S. Jones, E. Wildermuth, S. Lazaratos, and S. Bauer, 2013. Case studies of using far and ultra-far seismic data in deep-water Nigeria Erha North field: Beauty and the Beast. *International Petroleum Technology Conference*, March 26-28, Beijing, China, 5 p.